

## Enhancing Hydrocarbon Estimates in a Deepwater Turbidite Sequence

Rick Nelson, BP; Jean-Baptiste Clavaud, Chevron Technology Corp.; and Udit Kumar Guru and Hanming Wang, Schlumberger

Thinly laminated formations can be significant hydrocarbon reservoirs, particularly in turbiditic and fluvial environments. However, often such formations exhibit low resistivities when measured with conventional resistivity tools. These are known in the literature as classical low-resistivity pay and often are anisotropic in resistivity. Over the past decade, studies have shown that electrical anisotropy greater than three in these layered formations is caused by thin water-bearing beds, such as shale layers, alternating with the oil sands. Initial laboratory studies have shown that alternating variations in water saturation is a major contributor to resistivity anisotropy, but detailed laboratory research is needed before this can be generalized to all shaly-sand reservoirs.

Since their introduction in the early 1950s, wireline induction tools measured mainly the horizontal resistivity ( $R_h$ ). Consequently, when confronted with a potential

reservoir containing thinly laminated sand/shale sequences, it was a challenging task to decipher the thin hydrocarbon-bearing sands in the apparent low-resistivity hydrocarbon-bearing layer. The low-resistivity reading had to be corrected, usually by adding a shale-contribution term using one of the many published equations. More recently, technologies have been developed to measure the vertical dimension of this resistivity problem, or the vertical resistivity ( $R_v$ ), which can be evaluated using three tools: logging-while-drilling resistivity tools when the apparent angle between the tool and the formation is high; joint inversion of array laterolog and array-induction; and the triaxial induction tool, the focus of this article.

### North Africa Case Study

In a North Africa well, array-induction, nuclear magnetic-resonance (NMR), and nuclear (density-neutron and gamma ray) tools were run initially. The target interval was a deep-water turbiditic levee/overbank deposit, consisting of highly organized thin layers of high-quality gas-bearing sands. Layer thicknesses ranged from almost a meter to less than a centimeter, with most of the layers being in the centimeter range. The logged well encountered two gas-filled channel systems separated by a pressure barrier (Fig. 1). The lower system was a more proximal levee/overbank facies, of which the reservoir portion was made up of organized layers of high-quality coarse-grained sand interbedded with shales and some mudstones. Conversely, the upper system consisted of a levee/overbank facies having thin layers of finer-grained sands with shales and small amounts of mud.

Regular array-induction logs did not show noticeable invasion profile in this formation. The porosity (including clay-

**Rick Nelson**, SPE, is a petrophysical consultant in exploration for BP in Cairo. His areas of technical expertise include operations petrophysics, coring and core analysis, seismic rock properties, and general petrophysical integration. Previous BP assignments included working at BP's London Sunbury campus, working in its Azerbaijan Business Unit, and working with the Houston Technology Group. Previously, he was with Schlumberger (GeoQuest) and Oryx Energy. Nelson earned a BS degree in engineering sciences from Johns Hopkins U. **Jean-Baptiste Clavaud**, SPE, is a research petrophysicist with the Formation Evaluation Development team of Chevron Technology Corp. His areas of technical expertise include formation evaluation, special core analysis, resistivity interpretation, and petrophysical workflow design. Previously, he worked for Schlumberger both in scientific research at Schlumberger Doll Research and in development at the Sugar Land Product Center. Clavaud earned a PhD degree in geophysics from the U. of Paris. **Udit Guru**, SPE, is the Formation Evaluation and Solution Manager with Schlumberger in India. Previously, he was Petrophysics Domain Champion with Schlumberger, Egypt, where he was responsible for interpretation development and Egypt-based client support. He has 15 years of prior work experience with a national oil company. Guru earned an MS degree in exploration geophysics from the Indian Inst. of Technology, Kharagpur. **Hanming Wang**, SPE, is a senior engineer with Schlumberger in Sugar Land, Texas. His areas of technical expertise include well logging modeling, inversion, and log analysis. Wang earned a PhD degree in electrical engineering from the U. of Houston.

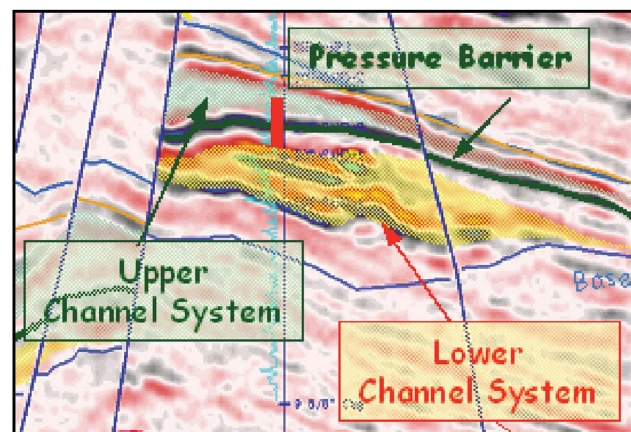
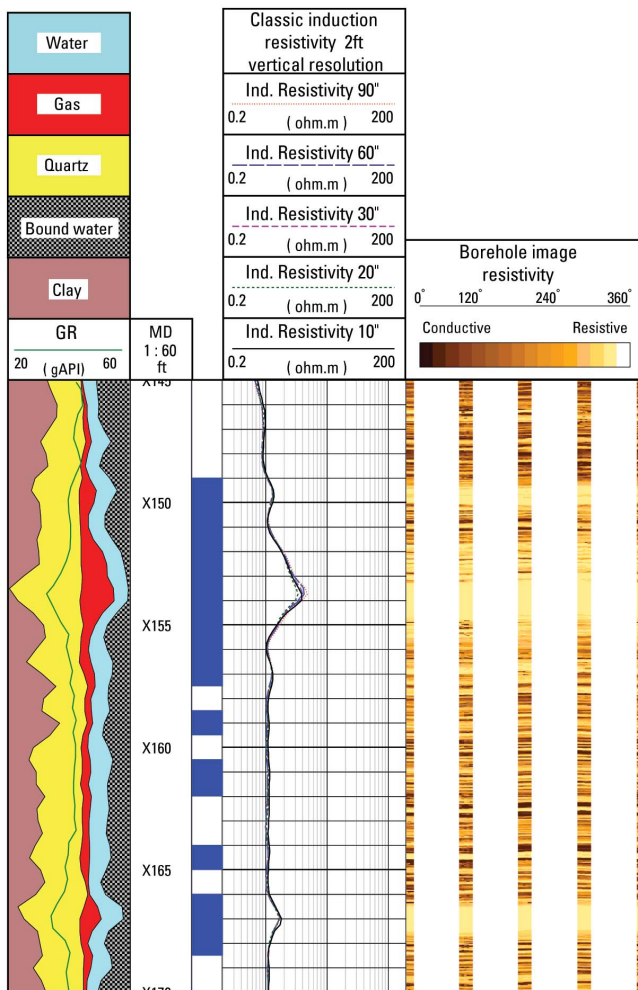


Fig. 1—Seismic cross section of the formation logged. Cored interval marked in red and  $F_{shale}$  in light blue.



**Fig. 2—Laminated sand analysis results of the triaxial induction tool resistivity anisotropy measurements. Track 1: sand/shale fraction; Track 2: depth; Track 3: GR column; Track 4: neutron and density; Track 5:  $R_v$  and  $R_h$ ; Track 6:  $S_w$ ; Tracks 7 and 8: pay flag for classic and anisotropy interpretation; Tracks 9 and 10: fluid volume for classic and anisotropy interpretation; Track 11: borehole image (resistivity).**

bound water) was 35%, and the effective porosity (without clay-bound water) was 25%. The separation between density and neutron showed a high amount of shale except in three places (X150–X155 ft, X188–X192 ft, and X268–X271 ft), where the cross-over between density and neutron indicated gas, also confirmed there by the higher resistivity measured by the regular induction log (Fig. 2). From the deep array-induction log, water saturation ( $S_w$ ) was computed with a dual-water equation to correct for clay conductivity. The data analysis, based on the array-induction tool and a dual-water shaly-sand approach, led to unreasonably high water saturations, with all resulting  $S_w$  values being close to unity, except in the three higher resistivity depths.

The horizontal resistivity of about 1–2  $\Omega\cdot\text{m}$  in this 30%-porosity formation was an example of classical low-resistivity pay. Borehole images also indicated the presence of thin shale

layers. The low conductivity of these shale laminae was the reason for this formation's low-resistivity reading. A high anisotropy was measured because this part of the reservoir consisted of these organized layers of high-quality hydrocarbon-bearing sands interbedded with shales and mudstones. In addition, the borehole images confirmed that the bed thickness was much smaller than the vertical resolution of the regular induction tool. Furthermore, photographs of the core taken confirmed the thinly laminated nature of the reservoir and that the sand layers were as thin as 1 cm in this section of the well.

This fluvial system with the thin-bedded sand/shale sequence presented the low-resistivity pay environment that made this well a good candidate for triaxial-induction use and the laminated-sand/shale analysis. As a result, the decision was made to test the fully triaxial multiarray induction tool, the RT Scanner, which uses a 1D inversion algorithm to provide  $R_v$  and  $R_h$  estimates around the wellbore. The  $R_v$  and  $R_h$  values, overlaid on top of the borehole image, showed good agreement between the lamination and the high-resistivity anisotropy.

Comparing the formation dip values with those obtained from borehole images showed good agreement, with both the magnitude and direction of each being consistent. Seismic data near this interval also indicate a dip consistent with triaxial-induction results, which helped confirm the seismic models of channel direction and orientation.

### Laminated-Sand/Shale Model

A laminated sand/shale model with anisotropic shales was built based on the  $R_v$  and  $R_h$  values inverted with the 1D code. Initially, the model was represented essentially as a formation of thinly laminated high-resistivity isotropic sands and low-resistivity anisotropic shales, with both components having similar porosities. Building the model used the following workflow.

- Build a two-component sand/shale volumetric system based on nuclear logs or NMR logs.
- Perform a petrophysical inversion of the resistivity anisotropy in terms of sand and shale resistivity ( $R_{\text{sand}}$  and  $R_{\text{shale}}$ ) incorporating anisotropic shale.
- Conduct a petrophysical interpretation and compute  $S_w$  for sand and for shale.
- Combine the two saturations into a final resistivity-anisotropy shaly-sand interpretation.

Two fundamental equations define the horizontal and vertical resistivities, forming what is known as the tensor anisotropy model. Because induction tools measure low-resistivity values in vertical and deviated wells, pessimistic interpretations of hydrocarbon volume result. For this well, the thickness of the sand/shale laminations is less than the about 1-ft vertical resolution of induction. The induction current loops pass through the horizontal layers in parallel. Therefore, on the one hand, the horizontal resistivity,  $R_h$ , is defined as:

$$R_h = \frac{R_{\text{sand}} \times R_{\text{shale}-h}}{(1 - F_{\text{shale}}) \times R_{\text{shale}-h} + F_{\text{shale}} \times R_{\text{sand}}}$$

The vertical resistivity,  $R_v$ , is defined as:

$$R_v = (1 - F_{shale}) \times R_{sand} + F_{shale} \times R_{shale-v}$$

It is apparent that the model is underdetermined with two equations and five unknowns:  $R_{sand}$ ,  $R_{shale-h}$ ,  $R_{shale-v}$ ,  $F_{shale}$ , and  $F_{sand}$ , so additional information is needed from other sources. A fraction-of-shale estimation can be provided from NMR logs or density-neutron logs, the latter of which was used from the classical interpretation for the shale-fraction input. Two of the unknowns ( $F_{shale}$  and  $F_{sand}$ ) are now fixed and are linked by the scalar expression:

$$F_{shale} + F_{sand} = 1.$$

With this expression, the linear system of equations involving  $R_v$  and  $R_h$ , described previously, can then be solved for  $R_{sand}$  and  $R_{shale-h}$ . Both of these equations contain as a model input the shale anisotropy ( $\alpha$ ). The shale anisotropy can be defined as the ratio of  $R_v$  to  $R_h$ . The range of the solutions may have to be controlled if the value chosen for  $\alpha$  does not match the log data. To determine the specific  $\alpha$  value from a log perspective, various field tests have been conducted, which found the shale-anisotropy ratio to be between 2 and 4. However, a representative value requires local calibration as well as some core measurements. In this case, the main thin-bedded reservoir has high-anisotropy resistivity values and is surrounded by shale at the top and bottom. A small distance down, there is one massive shale section where the anisotropy appears to be between 2 and 3, so a 2.5  $\alpha$  was used for the laminated sand/shale model. A composite plot of the laminated sand/shale interpretation is shown in Fig. 2. After  $R_{sand}$  and  $R_{shale}$  are computed based on  $R_v$ ,  $R_h$ ,  $F_{shale}$ , and  $\alpha$ , they can be linked to their respective saturations:

$$S_{wsand} = f_1(R_{sand}, \text{porosity}, R_w)$$

$$S_{wshale} = f_2(R_{shale}, \text{porosity}, R_w)$$

where  $f_1$  and  $f_2$  can be any resistivity-to-saturation transform (e.g., Archie's equation, the Waxman-Smiths model, or the dual-water model). Then, a volumetric average of the volume of fluid in each sand and shale component leads to:

$$S_{wt} = \frac{F_{shale} \cdot \phi_{shale} \cdot S_{w-shale} + (1 - F_{shale}) \cdot \phi_{sand} \cdot S_{w-sand}}{F_{shale} \cdot \phi_{shale} + (1 - F_{shale}) \cdot \phi_{sand}}$$

If the shale porosity and sand porosity are similar, the equation can be reduced to:

$$S_{wt} \approx F_{shale} \cdot S_{wshale} + (1 - F_{shale}) \cdot S_{wsand}$$

### Laminated-Sand/Shale Model

With the laminated-sand/shale model, the very high resistivity anisotropy (up to 20) translated into much lower  $S_w$  than the conventional interpretation ( $S_w$  in Track 6 in Fig. 2). Compared with the average high 70% value from classic

**TABLE 1—RESERVOIR SUMMATION AND NET-TO-GROSS COMPUTATION FROM  $R_h$  ONLY (CLASSIC) TRIAXIAL INDUCTION AND LAMINATED-SAND ANALYSIS, AND FROM CORE/BOREHOLE-IMAGE DATA (CORE/IMAGE).**

Model	Classic	Laminated-Sand	Core and Image
Top (ft)	X140	X140	X142.5
Bottom (ft)	X300	X300	X152.5
$F_{shale}$ cutoff, %	55	55	#
$\Phi$ cutoff, %	8	8	#
$S_w$ cutoff, %	70	60	#
Gross (ft)	160	160	#
Net (ft)	19	70	#
Net/Gross, %	12	44	50
Pay $\langle \Phi \rangle$ , %	28	25	30
Pay $\langle S_w \rangle$ , %	60	35	22
Gas pore volume			
% thickness (ft)	2	8	#

Note: The symbol  $\langle \rangle$  denotes average values.

interpretation ( $R_h$  only), the  $S_w$  derived from the triaxial-induction tool and the laminated-sand/shale model ( $R_v/R_h$ ) in the net part of the reservoir was about 30% (Table 1). In the main reservoir, where this anisotropy is the highest,  $S_w$  was about 80–100% (except at the depth X155 ft) for the classical, which was lowered to about 30% after the sand/shale analysis. These new  $S_w$  values obtained using the resistivity-anisotropy analysis were in good agreement with NMR diffusion-editing logs. Wireline formation-pressure testing and sampling operations indicated the layers to be in communication, and a drillstem test confirmed the producibility and provided a minimum indication of the reservoir extent.

Core also was obtained, with the cored section being predominantly in the upper channel system. The sealing facies, in the very bottom of the core, penetrated slightly into the lower, more proximal system. Core measurements showed an average  $S_w$  of 22%. Additionally, laboratory capillary pressure curves were performed on core taken from an adjacent well in the same formation. Using a previously published approach, the analogous capillary pressure data were simply arranged in terms of height above the free-water level and porosity. Analogous Dean-Stark direct-water saturation-measurements data show an average water saturation of about 26% in the net part of this reservoir. Therefore, measurements on both field and analogous core resulted in  $S_w$  values much closer to the 30% value derived from the laminated-sand/shale model than the conventional interpretation of 70%. Along with supporting  $S_w$  values, this subsequent core description and core analysis also have shown, likewise with the borehole images, that the interpreted section was indeed a high-quality thinly laminated reservoir, further confirming the additional hydrocarbon previously identified and the laminated-sand/shale model.

**TABLE 2—FOR THE MAIN RESERVOIR AND AN UPPER SECTION,  $R_{sand}$ ,  $R_{shale}$ , AND  $S_w$  ARE PRESENTED FOR TWO SHALE ANISOTROPIES (1 AND 2.5)**

Model	Main	Main	Upper	Upper
Top (ft)	X150	X150	X100	X100
Bottom (ft)	X175	X175	X140	X140
Shale anisotropy	1	2.5	1	2.5
$R_v$	23	23	2.3	2.3
$R_h$	1.3	1.3	0.7	0.7
$F_{shale}$	0.35	0.35	0.75	0.75
$\langle R_{sand} \rangle$	5.5	4	32	31
$\langle R_{shale} \rangle$	0.6	0.38	0.35	0.4
$\langle S_w \rangle$	0.4	0.35	0.55	0.9

Note: The symbol  $\langle \rangle$  denotes average values

In addition to the quantitative  $S_w$  computation, other properties derived from resistivity anisotropy also can aid the estimation of net-to-gross ratio. Using  $R_h$  only,  $R_v$  and  $R_h$ , and core data, three computations for the ratio of net-to-gross pay were performed. The net to gross was about 50% using core analysis (visual count). The net-to-gross-pay ratio computed from the resistivity anisotropy was near that of the core at about 45%, while the net to gross of the classic interpretation was not even close at 12%. From this conventional analysis, the reservoir summation calculated a small net reservoir thickness of about 20 ft compared to a 160-ft gross, assuming an 8% porosity cutoff, 55%  $F_{shale}$ , and 70%  $S_w$ . However, the new reservoir summation led to the much smaller average  $S_w$  and thus a much larger (70 ft) net thickness.

### Other Questions, Answers

While shale anisotropy is a parameter of the model, the question arises as to whether it is really needed. To answer this, forward modeling was performed of a laminated 50:50 sand/shale sequence with the same porosity, with and without shale anisotropy. The modeling analysis found that neglecting the shale anisotropy led to an overly optimistic  $S_w$  calculation, particularly in the transition zone or a water-wet sand, which led to an overestimation of hydrocarbon content. This also was confirmed in the laminated-sand/shale model. In fact, the effect of disregarding shale anisotropy is stronger in areas having moderate resistivity anisotropy (3–5). To illustrate this, two different volumes of gas were computed with the laminated-sand/shale model, by setting the  $\alpha$  value first to 2.5 and then to 1. There was not a strong effect at the top of the reservoir. However, stronger effects occurred in places having moderate  $R_v/R_h$  (3 to 4), such as those having increased shale content or high irreducible  $S_w$ . Consequently, in a shaly interval or in the transition zone, the computed  $S_w$  might be impaired.

Therefore, analyses of the data provided through the forward-modeling results, along with this example and other published cases, suggest that shale anisotropy plays a key

role in laminated-sand/shale model. Interpretation of anisotropy resistivity will be greatly influenced by shale anisotropy, which confirms the importance of including shale anisotropy for the interpretation of low-resistivity pay in laminated-sand/shale formations.

However, one of the big drawbacks of any petrophysical analysis using resistivity anisotropy is that it has a tendency to increase the hydrocarbon content dramatically. For this reason, the shale-anisotropy effect must always be handled explicitly. Laboratory work is required to better understand the variation from one type of shale to another. Otherwise, it will lead to poor reservoir-evaluation and -management decisions. Moreover, a thorough analysis of such a complex reservoir requires more than resistivity anisotropy. The borehole images and NMR data were key in this interpretation and for understanding the results.

Additionally, it has been shown that the resistivity anisotropy relates qualitatively to the permeability anisotropy (when the formation is at irreducible water saturation). Laboratory core permeabilities were measured on some of the core in the upper section using the minipermeameter technique. Based on the point-by-point permeability data, a  $k_t/k_v$  curve was built, normalized to a maximum of 20 for this well, and plotted against the  $R_v/R_h$  ratio. Although there appeared to be a qualitative similarity between resistivity and permeability anisotropy, it was determined that more measurements were needed to confirm this at a larger scale. Such an analysis must take into account that permeability anisotropy is sensitive only to the sedimentary/porous-network structure, while resistivity anisotropy is sensitive to both the rock and the fluid type.

The laminated-sand/shale petrophysical model including anisotropic shales and based on  $R_v$  and  $R_h$  values from the triaxial-induction tool led to better  $S_w$  calculations, thereby enhancing the hydrocarbon estimation in this low-resistivity pay and reducing the uncertainty of the gas-in-place assessment. The  $S_w$  values computed with the new model agreed very well with NMR-derived saturation values using diffusion-editing techniques in addition to analogous-core  $S_w$  measurements and capillary pressure data. This case and ones like it illustrate the beginning of a paradigm shift in which the evaluation focus is not on detecting the thin beds by increased resolution, but on evaluating them quantitatively using measured bulk anisotropy. Novel multicomponent induction technology will become a necessary part of an evaluation program in these environments worldwide. JPT

### References

- Clavaud, J.-B., Nelson, R., Guru, U.K., and Wang, H. 2005. Paper SPWLA 384622, Field Example of Enhanced Hydrocarbon Estimation in Thinly Laminated Formation with a Triaxial Array-Induction Tool: A Laminated Sand/Shale Analysis with Anisotropic Shale. Prepared for presentation at the SPWLA 46th Annual Logging Symposium, New Orleans, 26–29 June.
- Barber, T. et al. 2005. Determining Formation Resistivity Anisotropy in the Presence of Invasion. Prepared for presentation at the SPE Annual Technical Conference and Exhibition, Houston, 26–29 September. SPE 90526.